Photonic Compressive Sensing System Based on 1-Bit Quantization for Broadband Signal Sampling

Yuxiang Cai, Xiaohu Tang, Yamei Zhang, *Member, IEEE*, Han Gao, Xiuyuan Sun, and Shilong Pan, *Fellow, IEEE*

***Abstract*—Photonic compressive sensing (PCS), a paradigm for broadband sparse radio frequency (RF) signal acquisition, is recognized for its ability to significantly reduce sampling rate. However, conventional PCS systems face several challenges, including high storage requirements, limited noise resistance, and increased energy consumption during sampling. Additionally, they often struggle to accurately reconstruct frequency non-sparse signals and typically fail to resolve the time-frequency characteristics of signals with long temporal durations. In this study, we propose and experimentally validate a novel 1-bit quantization PCS (1-bit PCS) framework. Our system employs dictionary learning and local compressive sensing algorithm, enabling the effective recovery of various signal types, such as multi-tone, step-frequency, and linear frequency modulation (LFM) signals across a wide frequency range of 0 to 5 GHz. The sampling rate achieved is 1 GSa/s, corresponding to a compression ratio of 10. With this system, not only can the time-domain waveforms and spectrum of signals be accurately recovered, but the time-frequency characteristics are also captured with precision. This makes the system highly promising for applications in resource-limited scenarios.**

***Index Terms*—1-bit quantization, photonic compressive sensing (PCS), random demodulation.**

I. Introduction

ANALOG-TO-DIGITAL Converters (ADCs) play a paramount role in modern communication, radar, and electronic warfare systems. It converts analog signals to the digital domain and follows the Nyquist sampling law. However, the fast development of millimeter-wave technologies requires ADCs with high sampling rates and broad instantaneous bandwidths, which brings a tremendous challenge to the traditional ADCs. Additionally, the acquisition, storage, and processing of large amounts of signal data pose further difficulties. Fortunately, the compressive sensing (CS) theory provides a novel method that enables the sampling of high-frequency sparse signals at a significantly lower rate than the Nyquist sampling rate, recovering the signals accurately through reconstruction algorithms.

There are two primary structures referred to as random demodulation (RD) [1] and modulated wideband converter (MWC) [2]. Both systems have a similar structure consisting of five parts: signal mixing, low-pass filtering, low-speed sampling, quantization, and signal reconstruction. Initially, the sparse signal is multiplied with a pseudo-random binary sequence (PRBS) signal that alternates at a rate equal to or higher than the Nyquist sampling rate. This process ensures that the information contained in the sparse signal is distributed over the entire spectrum. Subsequently, a low-pass filter (LPF) is used to acquire the low-frequency component of the signal or to achieve signal integration. An electronic ADC with a sampling rate much lower than the Nyquist sampling rate will perform low-speed sampling and quantization. Ultimately, signal reconstruction is achieved through a CS algorithm in the digital signal processor (DSP). The total operational frequency range of the system is limited by the bandwidth of the mixing step among the five steps, leading to a high challenge when capturing broadband high-frequency signals since they have to mix with PRBS signals with symbol rates at or above the Nyquist sampling rate.

To address this issue, photonic CS (PCS) systems are proposed based on techniques such as photonic mixing [3], photonic integration [4], and microwave photonic filters [5], thanks to the significant benefits of the photonics technologies associated with large bandwidth, low loss, and immunity to electromagnetic interference [6]. Ref. [4] describes the construction of a photonic RD system using two cascaded Mach-Zehnder modulators (MZMs). This system efficiently mixes sparse signal with PRBS signal in the optical domain, allowing for the reconstruction of a 1-GHz single-tone signal with a sampling rate of 500 MSa/s. Nevertheless, due to the nonlinearity of the system, the output of the cascaded MZMs contains not only the harmonics components of the input signals but also the mixing spurs. Therefore, it is necessary to pre-measure the system parameters of the optical link and eliminate the effects through subsequent data processing, which would make the system bulky and complex. The solution to this problem involves the use of balanced detection [7], [8], multi-modulator cancellation [9] and single dual-electrode MZM photonic mixing [10]. Since the PRBS signal has undesirable characteristics, such as sloped edges and amplitude jitters, it can decrease the recovery performance of

Received 27 September 2024; revised 1 June 2025 and 10 July 2025; accepted 8 August 2025. Date of publication 18 August 2025; date of current version 2 October 2025. This work was supported in part by the Jiangsu Natural Science Foundation under Grant BM2022017, in part by the Fundamental Research Funds for the Central Universities under Grant NI2023003, in part by the Postgraduate Research & Practice Innovation Program of Jiangsu Province under Grant KYCX24_0585, and in part by the Fundamental Research Program for Young Student of National Key Laboratory of Microwave Photonics under Grant 24-JSKY-ZZKT-QNXS-15. *(Corresponding author: Yamei Zhang.)*

The authors are with the National Key Laboratory of Microwave Photonics, Nanjing University of Aeronautics and Astronautics, Nanjing 211106, China (e-mail: zhang_ym@nuaa.edu.cn).

Color versions of one or more figures in this article are available at https://doi.org/10.1109/JLT.2025.3599903.
Digital Object Identifier 10.1109/JLT.2025.3599903

the system. It can be solved by using optical pulses as a light source [11] or reducing the amplitude of the PRBS signal [12].

It should be noted that, the utilization of CS would decrease the signal-to-noise ratio (SNR) of the system, so the RIN noise introduced by the laser, the shot noise introduced by the photodetector (PD), and the thermal noise introduced by the electrical amplifier would affect the accuracy of the final reconstructed signal, which is an urgent problem to be solved in the PCS system [13]. Reference [14] proposed a 1-bit quantization method and established a mathematical model. The effectiveness of this method is verified by simulation. This method completely discards the amplitude information, retaining only the symbol information. Compared to amplitude variations, system noise makes it more difficult to reverse the signal symbols, resulting in improved noise immunity for the system. The 1-bit quantization method can also alleviate the problems of large storage pressure, high power consumption, and long processing time brought by the high-precision quantization of high-speed signal [15]. Moreover, 1-bit quantization data can greatly reduce the memory occupation and computational energy consumption of data processing [16]. It is expected to promote the development of miniaturization and integration of the PCS system. Currently, most of the research mainly focuses on mixing the sparse signal with the PRBS signal, and subsequent processes such as low-pass filtering and low-speed sampling are realized by computer post-processing, which do not provide a good exploration of the complete PCS system. In addition, most of the previously reported PCS systems can only reconstruct sparse multi-tone signals and are incapable of handling non-sparse signals in the frequency domain. The photonic MWC has the ability to process signals in multiple frequency bands [17], [18], but its construction is more intricate. Time delay errors and amplitude gain mismatches between each channel can compromise the accuracy of the recovered signal.

We have presented a 1-bit PCS system for multi-tone signal sampling in previous work [15]. In this paper, we have not only expanded the bandwidth of the system but also added processing methods to realize more complex signal sampling. A 1-bit PCS system for non-sparse signal reconstruction is proposed and experimentally demonstrated based on 1-bit quantization with dictionary learning and the local compressive sensing method. The system efficiently resolves the issues of high precision quantization mentioned before and enhances noise immunity. The dictionary learning is employed to find the sparse representation of the non-sparse signal, which can be further captured and reconstructed by the 1-bit PCS system. Local compressive sensing converts single long signal recovery to multiple short signal recovery, reduces the computability requirement of signal recovery, and can capture the time-frequency characteristics of the signal. A comprehensive experimental system is established, with a dual-parallel dual-drive Mach-Zehnder modulator (DP-DDMZM) and a PD to achieve relatively pure mixing. Additionally, a LPF is used to integrate the mixed signal. The impulse response of the LPF is experimentally measured by using the *m*-sequence excitation method. The proposed system successfully recovers a range of signals, including multi-tone signals, step-frequency signals, and LFM signals, throughout the frequency range of 0 to 5 GHz with only 1 GSa/s sampling rate and 1-bit quantization, corresponding to compression rate 10.

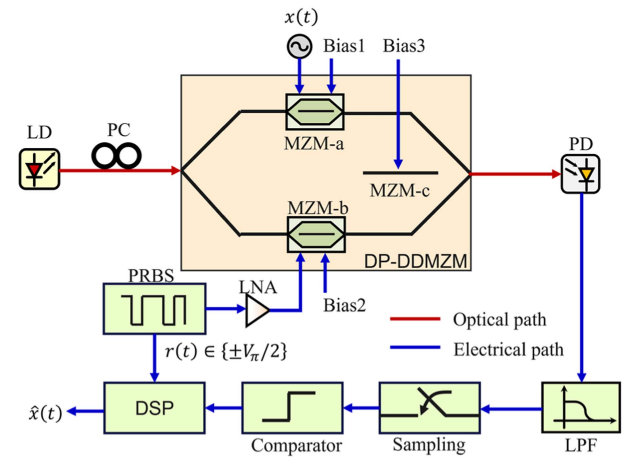

Fig. 1. Diagram of 1-bit PCS system structure. LD: Laser Diode; PC: polarization controller; DP-DDMZM: dual-parallel dual-drive Mach-Zehnder modulator; PD: photodetector; LPF: low-pass filter; DSP: digital signal processor; LNA: low noise amplifier.

II. Principle

A. 1-bit PCS Structure

Fig. 1 illustrates the schematic diagram of the proposed 1-bit PCS system, comprising five primary stages: photonic mixing, low-pass filtering, low-speed sampling, 1-bit quantization, and signal reconstruction. A continuous-wave (CW) optical carrier expressed as $E_{\text{in}}(t) = E_0 e^{j\omega t}$ is generated by a narrow linewidth laser and is then sent to a DP-DDMZM via a polarization controller (PC), where E_0 is the amplitude and ω is the angular frequency of the optical carrier. Two sub-DDMZMs embedded in a DP-DDMZM are followed to carry the RF signal $x(t)$ and the PRBS signal $r(t)$, respectively. The output of the DP-DDMZM can be expressed as,

$$E_{\text{out}} = \frac{1}{4} E_{\text{in}}(t) \left\{ \left(e^{j\Phi_x} + 1\right) + \left(e^{j\Phi_r} + 1\right) e^{j\Phi_{\text{dc}}} \right\} \quad (1)$$

where $\Phi_x = \pi(x(t)+V_{\text{a}}))/V_\pi$, $\Phi_r = \pi(r(t)+V_{\text{b}}))/V_\pi$, $\Phi_{\text{dc}} = \pi V_{\text{c}}/V_\pi$. These are the phase shifts introduced by the input signals and the three bias voltages V_{a}, V_{b}, V_{c}. The two sub-modulators of the DP-DDMZM are biased at the quadrature transmission point (QTP) and the main modulator is biased at the minimum transmission point (MITP) such that $V_{\text{a}} = V_\pi/2$, $V_{\text{b}} = V_\pi/2$, $V_{\text{c}} = V_\pi$.

The signal in (1) is beating at the PD and the output photocurrent is,

$$\begin{aligned} I_{\text{out}}(t) &= E_{\text{out}}(t) \cdot E^*_{\text{out}}(t) \\ &= \frac{1}{8} E_0^2 \left(1 - \cos\frac{\pi}{V_\pi}\left(x(t) - r(t)\right)\right) \end{aligned} \quad (2)$$

Controlling the amplitude of the PRBS signal to be $V_\pi/2$ and employing an AC-coupled PD to reduce the influence of the DC term, (2) can be simplified as,

$$I_{\text{out}}\left(t\right) = \pm\frac{1}{8}E_0^2\sin\frac{\pi}{V_\pi}x\left(t\right) \tag{3}$$

Given that the amplitude of the input signal $x(t)$ is small enough, the outcome of the photonic mixing component can be rewritten as,

$$I_{\text{out}}\left(t\right) = \begin{cases} Ax\left(t\right)\ r\left(t\right) = -\frac{V_\pi}{2} \\ -Ax\left(t\right)\ r\left(t\right) = +\frac{V_\pi}{2} \end{cases} \tag{4}$$

where A is a constant that is associated with the amplitude of the input optical signal E_0 and the modulation coefficient π/V_π. In this stage, the RF signal and PRBS signal are mixed, resulting in the expansion of the spectral information of the signal throughout the whole bandwidth of the system.

The mixed signal is fed into the LPF for low-pass filtering, performing convolution of $I_{\text{out}}(t)$ and the impulse response $h(t)$ of the LPF. This process achieves the integration of the signal. The output signal is then sampled by a low-speed sampler, quantized by a comparator, and finally reconstructed by the DSP. Compared with conventional compressive sensing systems, 1-bit quantization retains only the 1-bit symbol information of the signal and discards the amplitude information. If the amplitude is greater than zero, it is recorded as 1, and if the amplitude is less than zero, it is recorded as -1.

B. Mathematical Modeling of 1-bit PCS System

The CS model of the 1-bit PCS system can be expressed as,

$$\mathbf{y}_{1\text{bit}} = \text{sign}\left(\mathbf{DHRx}\right) = \text{sign}\left(\boldsymbol{\Phi\Psi\theta}\right) \tag{5}$$

where $\mathbf{x}$ is the discrete original signal of N×1 size sampled at Nyquist sampling rate. The discrete original signal $\mathbf{x}$ can be expressed as $\mathbf{x} = \boldsymbol{\Psi\theta}$, where $\boldsymbol{\Psi}$ and $\boldsymbol{\theta}$ are the transformation matrix and sparse vector, respectively. $\mathbf{D}$ is the down-sampling matrix of size $M\times N$ satisfying $D_{ij} = \delta(i\text{-}j/\text{R}_{\text{CS}})$, $i = 1,\ldots,M$, $j = 1,\ \ldots,N$. $\text{R}_{\text{CS}} = N/M$ is the compression ratio of the system, which measures the performance of the CS system, implying that the system is able to sample the signal and recover the original signal at a Nyquist sampling rate of $1/\text{R}_{\text{CS}}$. $\mathbf{H}$ is the LPF matrix related to the impulse response $h(t)$. $\text{R} = \{\pm 1\}$ is the symbol of the PRBS signal of the photonic mixing associated with the diagonal matrix of size $N\times N$. These three matrices are multiplied together to form a measurement matrix $\boldsymbol{\Phi} = \mathbf{DHR}$ of size $M\times N$. The comparator quantizes the sampled signal by means of the sign$(\cdot)$ function to obtain values $\mathbf{y}_{1\text{bit}}$ of size $M\times 1$ containing only one bit of sign information.

Recovered signal can be obtained by solving the optimization problem [19],

$$\hat{\boldsymbol{\theta}} = \text{argmin}\|\boldsymbol{\theta}\|_1 \text{ s.t. } \mathbf{Y}_{1\text{bit}}\boldsymbol{\Phi\Psi\theta} \geq 0,\ \|\boldsymbol{\theta}\|_2 = 1 \tag{6}$$

The inequality of the restrictions, denoted as $\mathbf{Y}_{1\text{bit}} = \text{diag}\{\mathbf{y}_{1\text{bit}}\}$, is applied element-wise. Due to the complete elimination of amplitude information in 1-bit quantization, the reconstructed signal must be limited to the unit ball $\|\boldsymbol{\theta}\|_2 = 1$ to ensure the recovered signal maintains the same relative amplitude as the original signal.

C. Signal Reconstruction

To reconstruct the original signal in the CS optimization model, all matrices must be considered. The sampling matrix $\mathbf{D}$ is determined by the set sampling compression ratio so that is known. The symbol information of the PRBS signal is stored in the DSP system before sampling. The PRBS signal source needs to be synchronized with the ADC during sampling. Thus the matrix $\mathbf{R}$ is also known.

Additionally, we need to determine the LPF matrix $\mathbf{H}$ and the sparse transform $\mathbf{x} = \boldsymbol{\Psi\theta}$ of the original signal. Accurate reconstruction results hinge on the precise determination of these matrices.

Obtaining the LPF matrix requires measuring the impulse response of the LPF, which is a crucial procedure. The impulse response of a linear time-invariant system can be efficiently acquired using the m-sequence excitation method [20]. This involves calculating the cross-correlation and auto-correlation functions between the input m-sequence signal and the system's output signal. The impulse response can be written as,

$$h\left(t\right) = \frac{1}{R_{mm}\left(0\right)}R_{my}\left(t\right) \tag{7}$$

where $R_{\text{mm}}(0)$ is the auto-correlation function of the input signal when $\tau = 0$, and $R_{\text{my}}(t)$ denotes the cross-correlation function between the input signal and the output signal. This measurement method is straightforward and can be accomplished by multiplexing the PRBS source of the PCS system. Because the m-sequence is a kind of PRBS, the sampling rate of the resulting impulse response matches the rate of the PRBS used, which can significantly reduce the testing time.

If the signal to be recovered by the CS system exhibits sparsity in the frequency domain, the transformation matrix $\boldsymbol{\Psi}$ can be substituted with the inverse Fourier transformation matrix $\mathbf{W}$, which is then multiplied by a spectrum vector $\boldsymbol{\theta}$ of size $N\times 1$ [3]. Nevertheless, the conventional CS system encounters difficulties in reconstructing signal that lack sparsity, such as LFM signal. Dictionary learning provides a solution by finding a special transformation matrix $\boldsymbol{\Psi}$. This matrix is a kind of overcomplete dictionary, unlike the inverse Fourier transformation matrix, which makes $\boldsymbol{\theta}$ as sparse as possible in frequency domain. This method makes the original signal sparse in other projection domain.

The K-SVD algorithm can be used to obtain the overcomplete dictionary $\boldsymbol{\Psi}$, whose optimization problem can be represented as [21],

$$\min_{\boldsymbol{\Psi},\boldsymbol{\Theta}}\left\{\|\mathbf{X} - \boldsymbol{\Psi}\Theta\|_{\text{F}}^2\right\} \text{ s.t. } \forall i, \|\boldsymbol{\theta}_i\|_0 \leq T_0 \tag{8}$$

where $\mathbf{X}$ is a training set consisting of multiple training data $\mathbf{x}_i$, which is obtained through prior information. $\boldsymbol{\Psi}$ is an overcomplete dictionary such that each vector $\boldsymbol{\theta}_i$ of matrix $\boldsymbol{\Theta}$ is a sparse representation of $\mathbf{x}_i$, and T_0 is the sparsity constraint threshold.

After determining the LPF matrix $\mathbf{H}$ and the transformation matrix $\boldsymbol{\Psi}$, the signal can be recovered by the 1-bit CS algorithm in the DSP. Extensive efforts have been devoted to developing CS algorithms for 1-bit quantization in order to recover the original signal. The commonly used algorithms include the binary iterative hard thresholding (BIHT) algorithm [22], the gradient projection subspace pursuit (GPSP) algorithm [23], and so on.

In addition, when the signal to be recovered has a long duration, both the CS algorithm and the K-SVD algorithm encounter challenges such as excessive data, long computation time, and high computational complexity [24]. These lead to poor real-time performance and significant pressure on data storage. Meanwhile, it is difficult to observe the time-frequency characteristics of the signal and ensure the accuracy of the signal recovery through the global recovery of the signal. Therefore, we are inspired by the short-time Fourier transform to transform global compressive sensing into local compressive sensing. The local compressive sensing is to divide the signal to be recovered into multiple segments and sequentially reconstruct each segment using a sliding window approach. Multiple local signal recovery reduces computational complexity, making the system better suited for resource-limited applications with high real-time requirements. Additionally, it enables capturing the time-frequency characteristics of the entire signal.

III. Experiment And Discussion

An experiment is constructed based on the diagram depicted in Fig. 1 to validate the effectiveness of the proposed approach. A narrow linewidth laser (TeraXion, PS-NLL) is employed to generate an optical carrier with a central wavelength of 1550 nm. The optical carrier passes through a PC and is fed into a DP-DDMZM (Fujitsu, FTM7960EX) with a 3-dB bandwidth of 25 GHz and a half-wave voltage (V_π) of 4 V. The RF signal is generated by an arbitrary waveform generator (AWG, Keysight, M9502A), and the PRBS signal is generated by a bit error rate tester (Sinolink, SL3000A). A low noise amplifier (LNA, AT-Microwave, AT-LNA-0043-3504) is employed to amplify the PRBS to be $V_\pi/2$. An AC-coupled photodetector (PD, Finisar, XPDV2120RA) with a 3-dB bandwidth of 40 GHz and a responsivity of 0.65 A/W is used for the photoelectric conversion. An LPF (Mini-Ciruits, VLFX-500) with a passband of DC$\sim$500 MHz is used to integrate the mixed signal. An oscilloscope (Tektronix, DSA72004B) with a bandwidth of 20 GHz is used for signal observation and low-speed sampling. The signal is recovered in the DSP using 1-bit quantization data processed offline.

A. System Construction and Impulse Response Measurement

To validate the photonic mixing results, a 100-MHz sine signal and a 10-Gbps PRBS signal are simultaneously fed into the DP-DDMZM. The output signal from the PD is analyzed by adjusting both the amplitude of the PRBS signal and the bias voltage of the modulator. By fine-tuning these parameters, the PD output is observed to reflect the mixing result. Fig. 2(a) displays the input sine signal, and Fig. 2(b) shows the PRBS signals. The mixing results of the PD output can be observed in Fig. 2(c). As can be seen from the figure, the output signal of the PD exhibits the opposite sign compared to the result of multiplying the sine signal with the PRBS signal, which aligns with the previously determined mixing model. Notably, the photonic mixing output is free from any irrelevant signals.

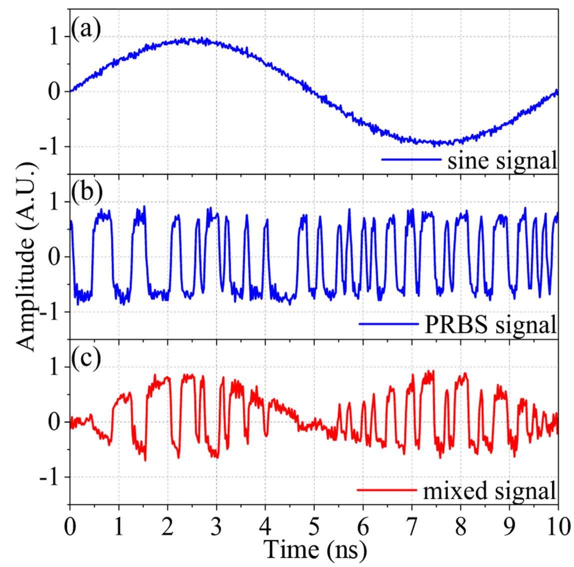

Fig. 2. Photonic mixing signal waveforms. (a) 100 MHz sine signal. (b) 10 Gbps PRBS signal. (c) Mixed signal from the output of the PD.

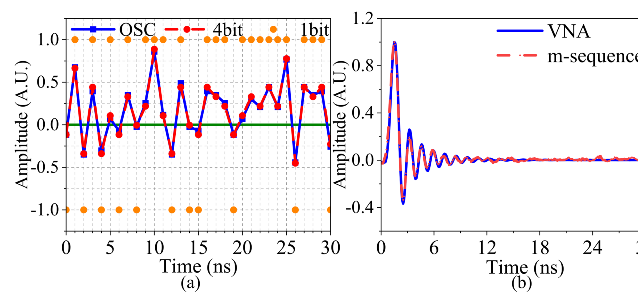

Fig. 3. (a) Data quantization after oscilloscope low-speed sampling. (b) LPF impulse response obtained by VNA and *m*-sequence excitation method.

Then, the signal under measurement is broadened across the entire spectrum through frequency mixing. An LPF with a passband of 500 MHz filters out the low-frequency components of the mixed signal, effectively integrating the signal. The final output is sampled at 1 GSa/s and quantized through offline processing, as shown in Fig. 3(a). While 4-bit quantization can retain more of the original signal information, 1-bit quantization only preserves the symbol information but significantly reduces the data storage requirements and speeds up the quantization process.

The impulse response of the LPF is determined by using the *m*-sequence excitation method, as shown in Fig. 3(b) (the red dashed curve). We also use a vector network analyzer (VNA, Keysight N5235A) to measure the amplitude response and phase response of the LPF. Then, the impulse response (the blue solid curve) is calculated by applying the inverse Fourier transform. The close agreement between the two curves demonstrates that the *m*-sequence excitation method is both convenient and effective for measuring impulse response.

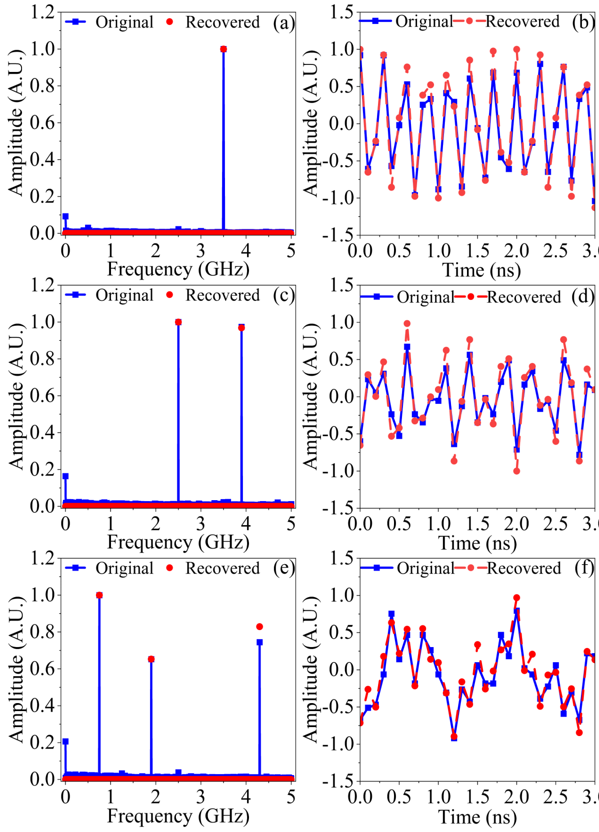

Fig. 4. Multi-tone signal oscilloscope sampling and recovery results. (a), (b) Spectrum and waveform of the 3.5 GHz. (c), (d) Spectrum and waveform of the 2.5 GHz and 3.9 GHz. (e), (f) Spectrum and waveform of the 0.75 GHz, 1.9 GHz, and 4.3 GHz.

B. Signal Reconstruction

All input signals for the experiments fall within the range of 0 to 5 GHz, with the PRBS signal mixed with the input signal at a rate of 10 Gbps. The sampling rate of the 1-bit PCS system is 1 GSa/s, and all sampling values are quantized to 1 bit.

According to the previously derived theory, the GPSP algorithm is employed to recover the original signal from 1-bit quantization values. The recovered signal is then compared with the results sampled at a Nyquist sampling rate of 10 GSa/s. Consequently, the system's compression ratio is 10.

For short-duration multi-tone signals that are sparse in the frequency domain, the inverse Fourier transformation matrix $\mathbf{W}$ is used as the transform matrix $\mathbf{\Psi}$. The signal sampling duration is 0.2 μs, with an amount of sampled $M = 200$ points and an amount of the signal to be recovered of $N = 2000$. Comparative experiments are carried out by acquiring and recovering a single-tone signal (3.5 GHz), a two-tone signal (2.5 GHz and 3.9 GHz), and a three-tone signal (0.75 GHz, 1.9 GHz, and 4.3 GHz) using both a 10-GSa/s oscilloscope and a 1GSa/s 1-bit PCS system. The results are presented in Fig. 4(a)–(f), respectively. The results indicate that the recovered signal closely matches the original signal, maintaining the same relative amplitude. This demonstrates the ability of the 1-bit PCS system to sample multi-tone signals effectively. Each original signal has a small DC component, which is likely due to the oscilloscope's internal circuits, so the recovery signal does not capture this DC component. For the 4.3 GHz component within the three-tone signal, there is a slight discrepancy, primarily attributed to information loss in 1-bit quantization and the reduced number of sample points for the high-frequency component compared to the low-frequency components during low-speed sampling. This problem can be solved by reducing the compression ratio of the 1-bit PCS system.

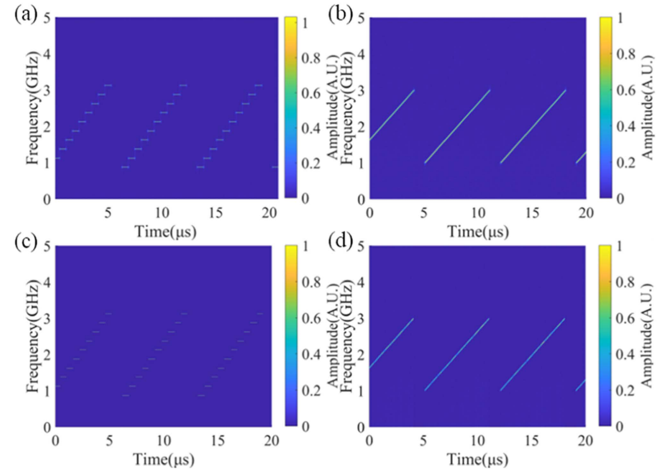

Fig. 5. Time-frequency diagrams. (a), (b) Oscilloscope-sampled step-frequency signal and LFM signal. (c), (d) Recovered step-frequency signal and LFM signal.

A long-duration step-frequency signal, commonly used in radar systems, is characterized by its time-varying frequency. It might be seen as a single frequency signal having a constant frequency over a specific duration. Thus, we also employ the inverse Fourier transformation matrix as the signal's transformation matrix. Fig. 5(a) is the original step-frequency signal with a central frequency of 2 GHz and a frequency interval of 0.25 GHz. The observation time length is 20 μs, which makes it difficult to recover the original signal and capture the time-frequency information using previous PCS systems. Fig. 5(c) shows the recovery results of compressive sampling of the step-frequency signal using local compressive sensing by the 1-bit PCS system. The length of the time window is 0.2 μs, with an amount of sampled $M = 200$ points and an amount of the signal to be recovered of $N = 2000$. It is evident that we are able to successfully recover the long-duration signal and precisely capture its time-frequency information. In addition, as a result of the CS method employed, only the value of the appropriate frequency is preserved, while all other frequency components are reduced to zero. Consequently, the recovered signal has a high SNR. The frequencies on the time-frequency diagram of the recovered signal are only straight lines, while the original signal has a certain width. This indicates that compressive sampling effectively recovers the original signal without introducing noise.

For long-duration LFM signals that are non-sparse in the frequency domain, the K-SVD algorithm is required to obtain the transformation matrix. The local compressive sensing is used

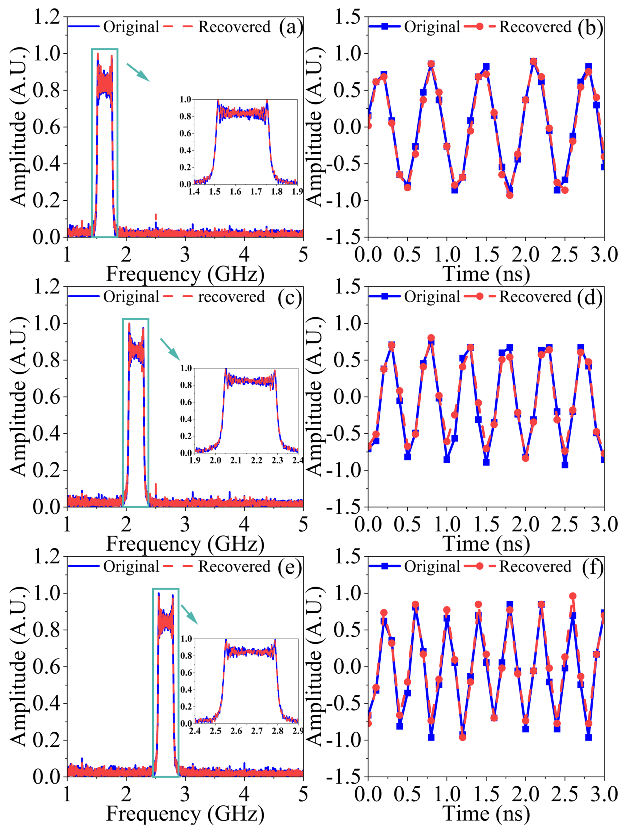

Fig. 6. LFM signal oscilloscope sampling and recovery results. (a), (b) Spectrum and waveform of the 1.5 GHz∼1.8 GHz. (c), (d) Spectrum and waveform of the 2.0 GHz∼2.3 GHz. (e), (f) Spectrum and waveform of the 2.5 GHz∼2.8 GHz.

to recover the entire signal, thereby reducing computational complexity and capturing the time-frequency characteristics of the signal. By applying dictionary learning, a sparse representation for non-sparse LFM signals in the frequency domain can be obtained. The inverse Fourier transformation matrix is substituted with the resulting overcomplete dictionary matrix. Fig. 5(b) depicts the original LFM signal, characterized by a central frequency of 2 GHz and a bandwidth of 2 GHz. The time length of the signal is 20 μs. The LFM recovered by the 1-bit PCS system using the local compressive sensing algorithm is shown in Fig. 6. It can be seen that the system is able to recover the signals in different frequency bands. The recovered signal exhibits minimal deviation from the original signal due to the presence of signals possessing identical characteristics in the overcomplete dictionary. Therefore, the utilization of the K-SVD algorithm and local CS algorithm in joint processing enables accurate recovery of non-sparse signals in the frequency domain. Fig. 5(d) represents the entire LFM signal that is recovered using the sliding window approach with local compressive sensing. The length of the time window is also 0.2 μs consistent with the recovery of the step-frequency signal. This approach effectively samples the LFM signal and captures its time-frequency information, significantly reducing computational complexity while ensuring accuracy in the recovered signal.

It is important to note that both signal time-frequency recovery results are recovered by using local compressive sensing, so their temporal resolution is determined by the length of the time window. The time window of the step-frequency signal can be tuned as long as the signal sparsity within each time window is fixed. However, the recovery of the LFM signal also relies on dictionary learning to provide the transformation matrix, and thus its time window length is fixed. The temporal resolution is determined at the time of acquiring the transform matrix and is related to the duration of the training data. If the recovered time window needs to be changed, a new transform matrix needs to be reacquired.

TABLE I
COMPARSION BETWEEN THE PROPOSED 1-BIT PCS SYSTEM AND 4-BIT PCS SYSTEM

	1-bit PCS	4-bit PCS
Single-tone SNR	28.36dB	28.36dB
Two-tone SNR	21.12dB	21.32dB
Three-tone SNR	19.58dB	19.96dB
step-frequency SNR	26.44dB	26.89dB
LFM SNR	21.23dB	21.23dB
Calculation time	14.2ms	10.5ms

C. Performance Analysis

Table I lists a comparison of the recovery accuracy of the 1-bit PCS and 4-bit PCS systems based on previous experimental results. The system performance is characterized by reconstructed SNR [22], given by,

$$SNR = 10\log_{10}\frac{\|x\|_2^2}{\|x-\hat{x}\|_2^2} \tag{9}$$

where x is the original signal, and $\hat{x}$ is the recovered signal. Since 1-bit quantization completely discards amplitude information, only the relative amplitude of the signal can be recovered. To compare the performance of the two systems, all reconstructed signals were normalized. The 4-bit quantization reconstructed SNRs are all better than 1-bit quantization except for single-tone signals and LFM signals. This is due to the fact that both signals only need to find a non-zero value in the recovery algorithm, and after normalization, both results are the same. Table I also shows the calculation times of the single-tone signals for the two systems. Obviously, the 1-bit PCS systems take longer to calculate, but both can fulfill the real-time requirements of the processing system.

Compared to 4-bit PCS systems, the 1-bit PCS system offers significant reductions in storage space and demonstrates superior performance in resource-limited scenarios. For the same amount of storage, the 1-bit quantization system stores only one-nth of the data required by the n-bit quantization system. We performed simulations to compare the performance of the 1-bit quantization system with the 4-bit quantization system under identical storage constraints.

The original signal is sampled at a rate of 10 GSa/s with a two-tone signal in the range of 0 to 5 GHz. The sampling time is 0.2 μs, and the number of sampling points is $N = 2000$. The experiment is repeated 300 times of signal recovery for all

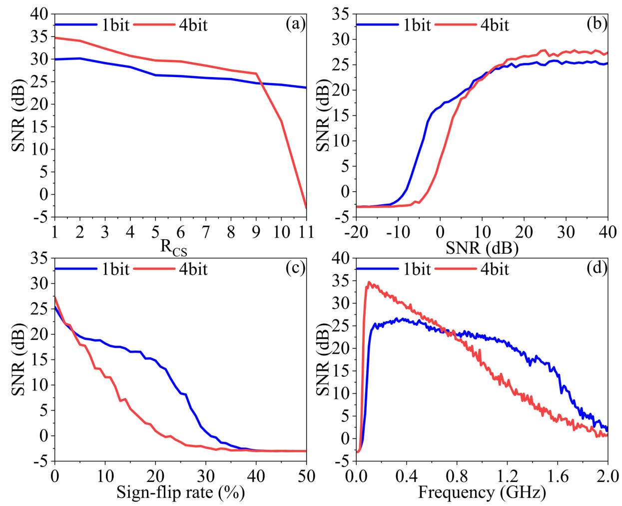

Fig. 7. (a) Performance at different compression ratios under the same bit budget. (b) Performance under varying input signal SNRs. (c) Performance with different quantization sign flip ratios. (d) Performance with different LPF cutoff frequencies.

the different values of the variables, and the average value of SNR is calculated. Since the reconstruction results are highly related to the compression ratio, we analyze the relationship between the SNR and the R_{CS} under the same bit budget as shown in Fig. 7(a). The horizontal coordinate in the figure is the 1-bit quantization R_{CS}. The R_{CS} of the 4-bit quantization corresponds to 4 times of the 1-bit quantization. When the 1-bit quantization R_{CS} is less than 9, the 4-bit quantization performs slightly better than the 1-bit quantization. However, as the compression ratio increases above 9, the performance of the 4-bit quantization system decreases significantly. The reason is that the compression ratio of the 4-bit quantization system is four times higher than that of the 1-bit quantization system, making it more challenging to recover the original signal at higher R_{CS} values. In order to fully represent the performance of the system, we choose $R_{CS} = 8$ in the next simulation, which means that the bit budget of all systems is $M = 250$ bits.

Then we evaluate the reconstruction performance of the system under different input SNRs. As shown in Fig. 7(b), the 4-bit quantization system performs a little better than the 1-bit quantization under high input SNR, while the 1-bit quantization significantly outperforms the 4-bit quantization under low input SNR. It means that 1-bit quantization has stronger noise immunity. It is also verified by the reconstructed SNR with different quantization sign flip ratios, as shown in Fig. 7(c). As the quantization bit sign is inverted, the SNR of 4-bit quantization decreases significantly, but 1-bit quantization decreases more slowly. This shows that 1-bit quantization is more robust and more stable.

In addition, the accuracy of the recovered signal is also related to the bandwidth of the LPF. Fig. 7(d) illustrates the SNR at different LPF cutoff frequencies. The results show that both too high and too low cutoff frequencies of the LPF will result in a lower SNR. This phenomenon is related to the integration effect of the LPF and the performance of the recovery algorithm. When the cutoff frequency is low, the LPF suppresses too much useful information, resulting in the recovery algorithm failing to accurately capture the sparse features of the original signal. At the same time, the impulse response amplitude of the LPF is too small, which also makes the mutual incoherence of the sensing matrix too large, leading to a low reconstruction SNR [25]. When the cutoff frequency is high, it exerts a more pronounced influence on the integrating function of the filter. And the signal passed by the filter already retains enough information for the recovery algorithm to be able to extract sparse features. Due to the high cutoff frequency of the LPF, the corresponding short integration time of the impulse response leads to a larger mutual incoherence of the sensing matrix. So the reconstructed SNR ratio is decreasing. Therefore, exploring how to select or construct appropriate LPFs is a topic for further research in the future.

Overall, the core advantages of the 1-bit PCS system lie in the extremely simple hardware, ultra-low power consumption and cost, as it requires only a simple comparator and is insensitive to analog front-end gain errors, providing strong noise immunity. However, its weakness is the large loss of quantization information, which results in a lower reconstruction accuracy than that of the 4-bit PCS system. And it requires more complex recovery algorithms, so the computation time is longer, but it can meet the real-time requirement. In contrast, the 4-bit PCS system significantly improves the reconstruction accuracy and reduces the algorithmic complexity by retaining more amplitude information. Nevertheless, it costs a significant increase in hardware complexity, power consumption, and cost, and has higher requirements for ADC accuracy and analog front-end linearity, which restricts its application in extreme low-power scenarios.

IV. Conclusion

In conclusion, we propose a 1-bit PCS system that can perfectly acquire multi-tone signals, step-frequency signals, and LFM signals. The problem of sampling high-frequency signals with limited storage space is solved. We successfully recovered multiple signals within 5 GHz with a sampling rate of 1 GSa/s and 1-bit quantization. With 1-bit quantization, the system is equipped with strong noise resistance, low data storage, high robustness, and low power consumption. Dictionary learning is used to enable the system to accurately capture non-sparse signals, such as LFM signals. Local compressive sensing solves the problems of high pressure on system signal recovery and difficulty in obtaining time-frequency features under long duration and large data volumes. These expand the application of the 1-bit PCS system. Experiments and simulations demonstrate the excellent performance of the system under the condition of limited resources. The proposed system is capable of potential applications in UAVs, robots, and other resource-limited, low-power scenarios.

References

[1] T. Ragheb, J. N. Laska, H. Nejati, S. Kirolos, R. G. Baraniuk, and Y. Massoud, “A prototype hardware for random demodulation based compressive analog-to-digital conversion,” in *Proc. 51st Midwest Symp. Circuits Syst.*, Knoxville, TN, USA, Aug. 2008, pp. 37–40.

[2] M. Mishali and Y. C. Eldar, “From theory to practice: Sub-Nyquist sampling of sparse wideband analog signals,” *IEEE J. Sel. Top. Signal Process.*, vol. 4, no. 2, pp. 375–391, Apr. 2010.
[3] J. M. Nichols and F. Bucholtz, “Beating Nyquist with light: A compressively sampled photonic link,” *Opt. Exp.*, vol. 19, no. 8, pp. 7339–7348, Apr. 2011.
[4] Y. Chen et al., “Compressive sensing in a photonic link with optical integration,” *Opt. Lett.*, vol. 39, no. 8, pp. 2222–2224, Apr. 2014.
[5] Y. Chen et al., “Photonic compressive sensing with a micro-ring-resonator-based microwave photonic filter,” *Opt. Commun.*, vol. 373, pp. 65–69, Aug. 2016.
[6] J. Yao, “Microwave photonics,” *J. Lightw. Technol.*, vol. 27, no. 3, pp. 314–335, Feb. 2009.
[7] F. Yin et al., “Multifrequency radio frequency sensing with photonics-assisted spectrum compression,” *Opt. Lett.*, vol. 38, no. 21, pp. 4386–4388, Nov. 2013.
[8] L. Yan et al., “Integrated multifrequency recognition and downconversion based on photonics-assisted compressive sampling,” *IEEE Photon. J*, vol. 4, no. 3, pp. 664–670, Jun. 2012.
[9] H. Chi et al., “Microwave spectral analysis based on photonic compressive sampling with random demodulation,” *Opt. Lett.*, vol. 37, no. 22, pp. 4636–4638, Nov. 2012.
[10] B. Yang, S. Yang, Z. Cao, J. Ou, Y. Zhai, and H. Chi, “Photonic compressive sensing of sparse radio frequency signals with a single dual-electrode Mach–Zehnder modulator,” *Opt. Lett.*, vol. 45, no. 20, pp. 5708–5711, Oct. 2020.
[11] W. Dai, B. Yang, S. Yang, Y. Zhai, J. Ou, and H. Chi, “Photonic compressive sensing of microwave signals with enhanced compression ratio and frequency range via optical pulse random mixing,” *Opt. Lett.*, vol. vol. 50, no.no. 2, pp. 261–264, Jan. 2025.
[12] S. Liu and Y. Chen, “Photonic random demodulator with improved performance by compressing the PRBS amplitude,” *IEEE Photon. Technol. Lett.*, vol. 36, no. 5, pp. 329–332, Mar. 2024.
[13] Y. Xu et al., “Random code shifting based ultra-wideband photonic compressive receiver with image-frequency distinction,” *Opt. Exp.*, vol. 31, no. 5, pp. 8725–8737, Feb. 2023.
[14] B. Yang, Q. Xu, H. Chi, Z. Liu, and S. Yang, “Photonic compressive sampling of wideband sparse radio frequency signals with 1-bit quantization,” *Opt. Exp.*, vol. 31, no. 11, pp. 18159–18166, May 2023.
[15] Y. Cai, X. Tang, Y. Zhang, and S. Pan, “Sparse radio frequency signal sampling based on 1-bit quantized photonic compressive sensing system,” in *Proc. Int. Topical Meeting Microw. Photon.*, Nanjing, China, 2023, pp. 1–4.
[16] H. Wang et al., “BitNet: Scaling 1-bit transformers for large language models,” arXiv: *2310.11453*.
[17] Y. Liang, M. Chen, H. Chen, C. Lei, P. Li, and S. Xie, “Photonic-assisted multi-channel compressive sampling based on effective time delay pattern,” *Opt. Exp.*, vol. 21, no. 22, pp. 25700–25707, Nov. 2013.
[18] H. Nan, Y. Gu, and H. Zhang, “Optical analog-to-Digital conversion system based on compressive sampling,” *IEEE Photon. Technol. Lett.*, vol. 23, no. 2, pp. 67–69, Jan. 2011.
[19] P. T. Boufounos and R. G. Baraniuk, “1-Bit compressive sensing,” in *Proc. 42nd Annu. Conf. Inf. Sci. Syst.*, Mar. 2008, pp. 16–21.
[20] M. Holters, T. Corbach, and U. Zölzer, “Impulse response measurement techniques and their applicability in the real world,” in *Proc. 12th Int. Conf. Digit. Audio Effects*, Como, Italy, 2009, pp. 108–112.
[21] M. Aharon, M. Elad, and A. Bruckstein, “K-SVD: An algorithm for designing overcomplete dictionaries for sparse representation,” *IEEE Trans. Signal Process.*, vol. 54, no. 11, pp. 4311–4322, Nov. 2006.
[22] J. N. Laska and R. G. Baraniuk, “Regime change: Bit-depth versus measurement-rate in compressive sensing,” *IEEE Trans. Signal Process.*, vol. 60, no. 7, pp. 3496–3505, Jul. 2012.
[23] S. Zhou, Z. Luo, N. Xiu, and G. Y. Li, “Computing one-bit compressive sensing via double-sparsity constrained optimization,” *IEEE Trans. Signal Process.*, vol. 70, pp. 1593–1608, Mar. 2022.
[24] R. Rubinstein, M. Zibulevsky, and M. Elad, “Efficient implementation of the K-SVD algorithm using batch orthogonal matching pursuit,” *CS Technion*, vol. 40, no. 8, pp. 1–15, Apr. 2008.
[25] M. Elad, “Optimized projections for compressed sensing,” *IEEE Trans. Signal Process.*, vol. 55, no. 12, pp. 5695–5702, Dec. 2007.